

DEGRADATION OF NANOPARTICULATE-COATED AND UNCOATED SULFIDE-BASED CATHODOLUMINESCENT PHOSPHORS

B.L. Abrams¹, W.J. Thomes¹, J.S. Bang² and P.H. Holloway²

¹Sandia National Labs, Albuquerque, P.O. Box 5800-1421, NM 87185, USA

²Department of Materials Science and Engineering, University of Florida, Gainesville, FL 32611-6400, USA

Received: July 02, 2003

Abstract. Changes in the cathodoluminescent (CL) brightness and in the surface chemistry of nanoparticulate SiO₂-coated and uncoated ZnS:Ag,Cl powder phosphor have been investigated using a PHI 545 scanning Auger electron spectrometer (AES), an Oriel optical spectrometer and a JEOL 6400 scanning electron microscope (SEM). The data were collected in a stainless steel UHV chamber with residual gas pressures between 1x10⁻⁸ and 1x10⁻⁶ Torr as measured by a Dycor LC residual gas analyzer (RGA). The primary electron current density was 272 μA/cm², while the primary beam energy was varied between 2 and 5 keV. In the presence of a 2keV primary electron beam in 1x10⁻⁶ Torr of water for both the SiO₂-coated and the uncoated cases, the amounts of C and S on the surface decreased, that of O increased and the CL intensity decreased with electron dose. This surface chemistry change lead to the development of a surface dead layer and is explained by the electron beam stimulated surface chemical reaction model (ESSCR). The penetration range of the impinging low energy primary electrons is on the order of 10-100 nm creating a reaction region very close to the surface. The ESSCR takes this into account postulating that primary and secondary electrons dissociate physisorbed molecules to form reactive atomic species. These atomic species remove surface S as volatile SO_x or H₂S. In the case of an oxidizing ambient (i.e. high partial pressure of water), a non-luminescent ZnO layer is formed. This oxide layer has been measured to be on the order of 3-30 nm. In the case where the vacuum of 1x10⁻⁸ Torr was dominated by hydrogen and had a low water content, there was a small increase in the S signal, no rise in the O Auger signal, but the CL intensity still decreased. This is explained by the ESSCR whereby H removes S as H₂S leaving elemental Zn, which evaporates due to a high vapor pressure.

In the case of ZnS:Ag,Cl coated with SiO₂, morphological changes were observed on the surface after extended electron beam exposure. Erosion of ZnS occurs more dramatically at an accelerating voltage of 5kV even at the same current density. Uncoated ZnS:Ag,Cl phosphors exhibited similar surface chemical changes to that of SiO₂-coated ZnS:Ag,Cl but did not degrade to the same extent. Also, no change in the surface morphology was observed. These SEM images as well as reaction rate data suggest that these nanometer sized SiO₂ particles acted as a catalyst for decomposition of the ZnS especially in a reducing ambient (i.e. high hydrogen partial pressure).

In order to reduce CL degradation of these and other phosphors, protective coatings were pulse laser deposited onto the phosphor surface. The effectiveness of these coatings was dependent upon both the thickness and the uniformity. Thicknesses of these coatings ranged from 1-5 nm and were uniform as determined using profilometry and TEM.

1. INTRODUCTION

There are several different degradation mechanisms that affect the luminescence of sulfide-based phosphors in the Field Emission Display (FED) environ-

ment. These mechanisms include electron beam stimulated surface chemical reactions (ESSCR) [1], vacuum ambient effects [1-3], temperature effects [4-6], charging [7] and surface morphology [2]. It is not known if these mechanisms operate concurrently

Corresponding author: B.L.Abrams, e-mail: blabram@sandia.gov

or separately. These mechanisms are especially prevalent in the FED due to its configuration. Operation of an FED is similar to the cathode ray tube (CRT) in that electron beam bombardment is used to produce cathodoluminescence (CL). However, the details and structure of the display are very different. The color CRT uses three electron beams with accelerating voltages of 25 kV. These electron beams are rastered across the phosphor screen to form an image. All this takes place inside of a vacuum tube with an approximate pressure of 1×10^{-6} to 1×10^{-7} Torr. On the other hand, the FED is composed of a cathode and an anode plate separated by a gap of only a few millimeters (0.1 to 3 mm) [8]. This small gap makes it difficult to obtain a good vacuum with low partial pressures of harmful residual gases, *i.e.*, H_2O , O_2 , CO_2 (see discussion below). The cathode, or backplate, side houses thousands of tiny (~ 40 -150 nm) field emitter tips organized in a matrix of row and column traces. There are as many as 4,500 emitters at each row/column union [8]. Electrons are emitted from these nanotips (made usually of molybdenum or silicon) by the application of a small voltage across the row cathode and column gate. The electrons strike the phosphor screen with low accelerating voltages between 0.5 to 6 kV. This is the cold cathode method of field emission and can be described by the Fowler-Nordheim equation. The anode, also known as the faceplate, is where the image is actually created. It is here that the phosphors are located and separated into the "picture elements", or pixels.

In order to aid in the success of FEDs, phosphors must uphold many requirements and properties over the lifetime of a display. Holloway *et al.* has outlined these critical parameters to be: brightness, chromaticity, efficiency, saturation, conductivity, particle size, particle composition and maintenance [9]. Included as subcategories of these parameters are morphology, stoichiometry, minimal temperature quenching, fast decay time, stability under heat treatment and surface characteristics [9]. Phosphor brightness must parallel or exceed that of the current CRTs and be on the order of 300 cd/m^2 . The color should be as saturated as possible. High energy conversion efficiency (power output as a function of power input: W/W) as well as high luminous efficiency (brightness output per unit input power (Lm/W)) are both essential [9]. Saturation of brightness, where brightness no longer increases as rapidly with increasing current, is undesirable. Particle size, composition and surface morphology for both the activator and the host material control the excitation properties of the material. All

of these properties come together in increasing the radiative recombination rate over and above the nonradiative rate [9-15].

The requirements imposed upon the phosphors become difficult to uphold in the FED device configuration. This is due to the fact that the low accelerating voltage used creates an excitation volume in the phosphor that is limited to the near surface region. Cathodoluminescent degradation of sulfide phosphors under these conditions was investigated by Swart *et al.* and Holloway *et al.* [1,3,7,9,12,16-18]. $ZnS:Cu$, Al , Au and $ZnS:Ag,Cl$ powder phosphors were bombarded by 2 kV electrons with a current density of 2 mA/cm^2 in two different vacuum ambients: 1.2×10^{-8} Torr residual gas and 1×10^{-6} Torr O_2 . Auger electron spectroscopy (AES) and CL measurements were taken simultaneously during a twenty four-hour electron beam exposure period. A correlation was made between CL decay and changes in the surface chemistry. Degradation left the phosphor surface depleted of sulfur and carbon and rich in oxygen. AES spectra showed a decrease in the S peak and an increase in the O peak, which is indicative of the formation of a ZnO surface dead layer. Holloway *et al.* and Swart *et al.* postulated that these surface chemistry changes were caused by electron beam stimulated surface chemical reactions (ESSCR) [1, 3, 7, 9, 12, 16]. They suggested that the electron beam dissociated surface adsorbed species such as H_2O and O_2 converting them into reactive atomic species. These reactive atomic species combined with S, forming products with high vapor pressure such as H_2S or SO_x , which would escape from the surface leaving behind an increasingly thick non-luminescent oxide (*i.e.*, ZnS to ZnO). Swart *et al.* estimated the thickness of the oxide layer to be 30E. However, in order to achieve the observed CL decay at 2 kV, Swart *et al.* speculated that the dead layer must be on the order of $\sim 100 \text{ \AA}$ based on electron interaction volume calculations [3]. Therefore, they concluded that the presence of the dead layer was not enough to explain the extent of the CL decay demonstrated. They then postulated that along with the ESSCR, subsurface point defects were being created which led to an increased probability of non-radiative recombination [3]. A mathematical model of the ESSCR was developed by Holloway *et al.* showing the dependence of degradation on gas type, gas pressure, current density and electron beam energy [1]. Since bulk properties are not operative in this degradation process due to the low electron energy used (as implied by Bechtel *et al.* [19]), Holloway's model incorporated a surface science

approach. With this model, the concentration of sulfur is predicted to decrease exponentially with coulomb load and CL loss rate will increase with increasing gas pressure [1].

As stated by the ESSCR model, gas pressure is an important factor in CL degradation. More specifically, the type of gas partial pressure was shown to play a vital role. When the vacuum ambient was oxidizing (i.e., high H_2O partial pressure of $\sim 1 \times 10^{-6}$ Torr), a nonluminescent oxide layer (i.e., ZnO) or "dead layer" formed. However, in a reducing ambient (i.e., high H_2 partial pressure $\sim 1 \times 10^{-6}$ Torr), S was removed by H_2 , presumably as H_2S , leaving elemental Zn to evaporate since it has a fairly high vapor pressure under these conditions [4,5]. If, during this process, the temperature of the phosphor is increased, then the evaporation rate of the elemental Zn will increase. This situation has been shown to arise when the electron beam power density is increased to values on the order of $\sim 1 \text{ W/cm}^2$ [2].

As a subsequent stage of CL degradation, following ESSCR and vacuum ambient effects, temperature has been shown to play a significant role. It manifests itself through thermal quenching of luminescence as well as in physical deterioration of the phosphor material. Itoh *et al.*, in studying the CL degradation as a result of a $ZnSO_4$ dead layer formation on $ZnS:Zn$ and $(Zn_{0.22}Cd_{0.78})S:Ag,Cl$, also observed morphological deterioration of his powder phosphors [20]. This was attributed to decomposition and evaporation of the phosphor grains. Electron beam heating was reported as the cause for this evaporation. More specifically, in the model of CL degradation of sulfide phosphors, Holloway *et al.* shows that there is a temperature dependence for ESSCR degradation [1]. For the assumed mechanism, degradation decreases and temperature increases, demonstrated by Swart *et al.* [6]. Most recently, Kajiwara *et al.* compared the effects of temperature on the CL luminous efficiency of P22 $ZnS:Ag,Al$ and P55 $ZnS:Ag,Al$ phosphors under a 10 kV $0.5 \mu\text{A/cm}^2$ electron beam. They reported that the temperature at which the efficiency is half that at room temperature, T_{50} , was 170 °C for the P22 and 230 °C for the P55. They attributed this difference to a higher defect concentration in the P22 phosphors as shown by TEM [21].

Many conditions and parameters play a role in CL degradation of sulfide-based phosphors. None of the degradation mechanisms occurs unless electron beam bombardment of the phosphor takes place. Of course, this is the very source of cathodoluminescence. Several researchers have attempted to reduce the effects of degradation by

either mixing the phosphor with another compound or protectively coating it. Kominami *et al.* mixed $ZnS:Ag,Cl$ with In_2O_3 and also applied a 10 nm thick layer of In_2O_3 to the $ZnS:Ag,Cl$ phosphor powder using the sol-gel method. The In_2O_3 coated phosphors were brighter as a result of the coating. They attributed this to the conductive properties of the coating, which decreased surface charging. The coating also improved aging characteristics. The mixture of ZnS with In_2O_3 did not fare as well. It actually resulted in a loss of brightness and had no effect on the aging properties [22,23]. Effects of coating with blue Cu_xS on $ZnS:Ag,Cl$ was investigated by Yang *et al.* They found that the CL intensity of the coated phosphor improved depending upon heat treatment conditions. Reduction of the CL intensity was observed if the coated phosphor was baked at high temperatures due to oxidation of the phosphor [24].

Lee *et al.* coated $ZnS:Ag$ with MgO and coated $Y_2SiO_5:Ce$ with In_2O_3 , Al_2O_3 and SiO_2 . They found that the CL efficiency was improved for the MgO -coated $ZnS:Ag$ and the Al_2O_3 and SiO_2 -coated $Y_2SiO_5:Ce$. However, the efficiency decreased for In_2O_3 coating of $Y_2SiO_5:Ce$ [25].

In this paper, the effects of nanoparticulate non-uniform coatings on sulfide-based phosphors (specifically ZnS) on degradation will be discussed. The relationship between the coating properties and other degradation mechanisms such as temperature, vacuum ambient as well as charging will also be discussed.

2. EXPERIMENTAL PROCEDURES

In order to study the CL degradation of $ZnS:Ag,Cl$, a simulated FED environment was created. This consisted of an ultrahigh vacuum (UHV) system equipped with an electron gun housed inside of a cylindrical mirror analyzer (CMA). This system allowed for simultaneous measurement of CL and Auger Electron Spectroscopy (AES). AES data was collected using a Physical Electronics (PHI) model 545 scanning Auger electron spectrometer. A cylindrical mirror analyzer (CMA) model 15-110 was used as the Auger electron detector and was mounted horizontally onto the vacuum system. Current to the electron gun filament was controlled using the electron gun control unit model PHI 11-045. The electron beam accelerating voltage was controlled by a PHI model 20-085 power supply with range capability between 0-10 kV. However, most of the experiments utilized either a 2 keV or a 5 keV primary electron beam energy.

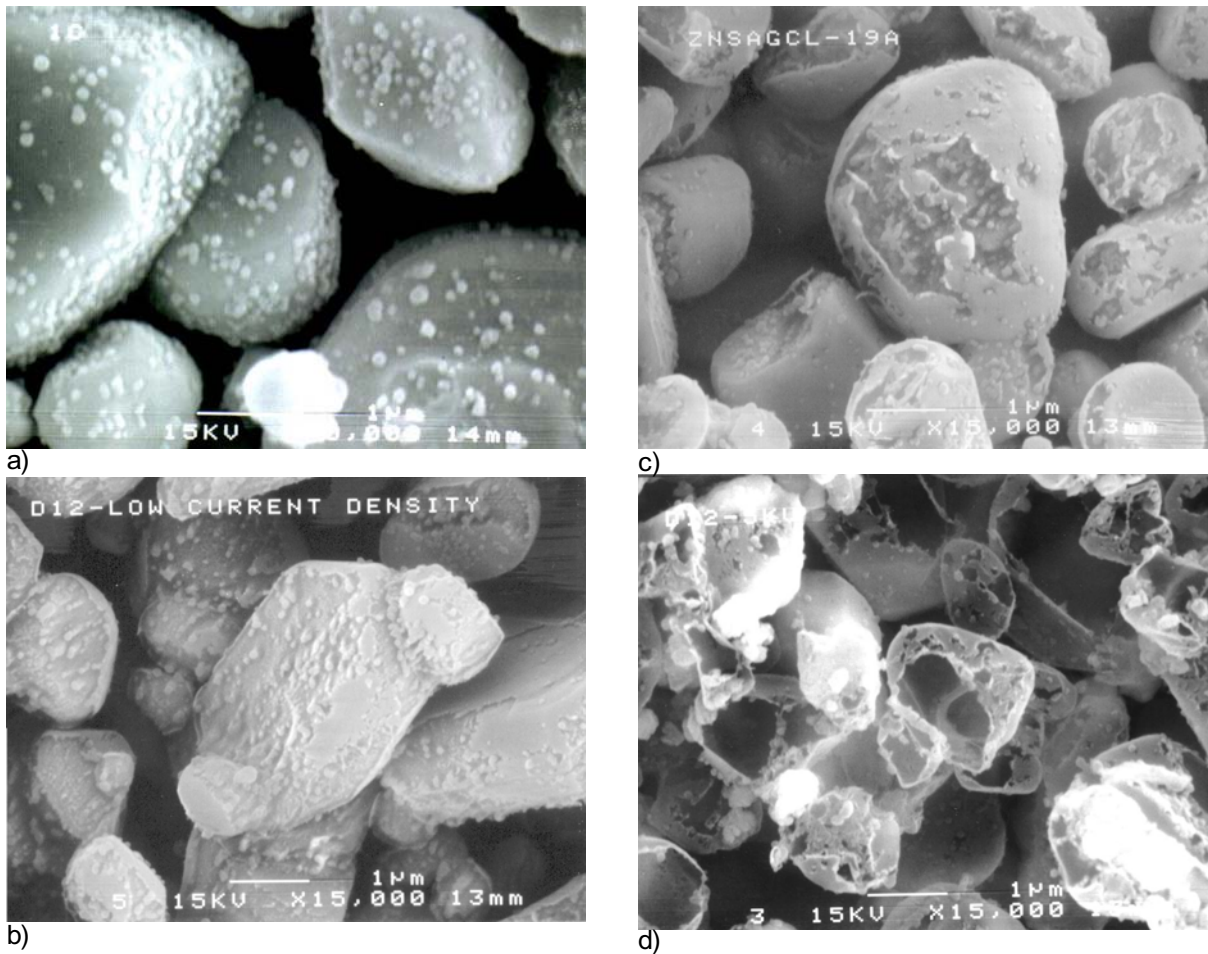


Fig. 1. SEM images of SiO_2 -coated $\text{ZnS}:\text{Ag},\text{Cl}$ powder phosphor (a) (top left) before degradation, (b) (top right) after degradation at 0.4 W/cm^2 , (c) (bottom left) after degradation at 0.6 W/cm^2 , (d) (bottom right) after degradation at 1.4 W/cm^2 .

The modulation voltage was maintained at 4 eV peak to peak on the Auger System Control unit model PHI 11-500A. This AES system utilized a PAR Model HR-8 lock-in amplifier as a detection system and all the data was collected in the $dN(E)/dE$ mode.

An Oriel Instaspec IV CCD detector with a 77400 Multispec Spectrophotometer/ Monochromator was used to collect CL spectra and measure the intensities. This CCD detector was mounted externally to the vacuum system and viewed the sample through a 4" zero length quartz view port. Two lenses were used to focus the light coming through the view port into the monochromator and subsequently to the CCD camera.

The scanning electron microscope used for this work was a JEOL 6400 SEM. Residual gas spectra were collected using a Dycor LC 100AMU series mass spectrometer from Ametek.

Powder $\text{ZnS}:\text{Ag},\text{Cl}$ phosphor was obtained commercially in two forms: with and without SiO_2

nanoparticulate coatings. SiO_2 coatings are typically used to ease handling of the phosphor during screen-printing onto the glass faceplate during the FED manufacturing process. Three different coatings were deposited using pulsed laser ablation (PLD) on the $\text{ZnS}:\text{Ag},\text{Cl}$ phosphor with no initial coating in an attempt to provide a protective layer. The phosphors were housed in a deposition vacuum chamber consisting of a fluidized bed. The purpose of this fluidized bed was to allow rotation of the phosphor particles during deposition in an effort to coat them uniformly. However, as will be seen below in the results section, uniform coatings were not obtained.

Phosphor powder samples were cold pressed into 1/16" deep, 1/8" wide holes of a stainless steel holder. These holders were mounted directly onto a carousel inside the main UHV chamber. Sample currents were measured by connecting the positive lead of a 62.7 V battery to the sample carousel via

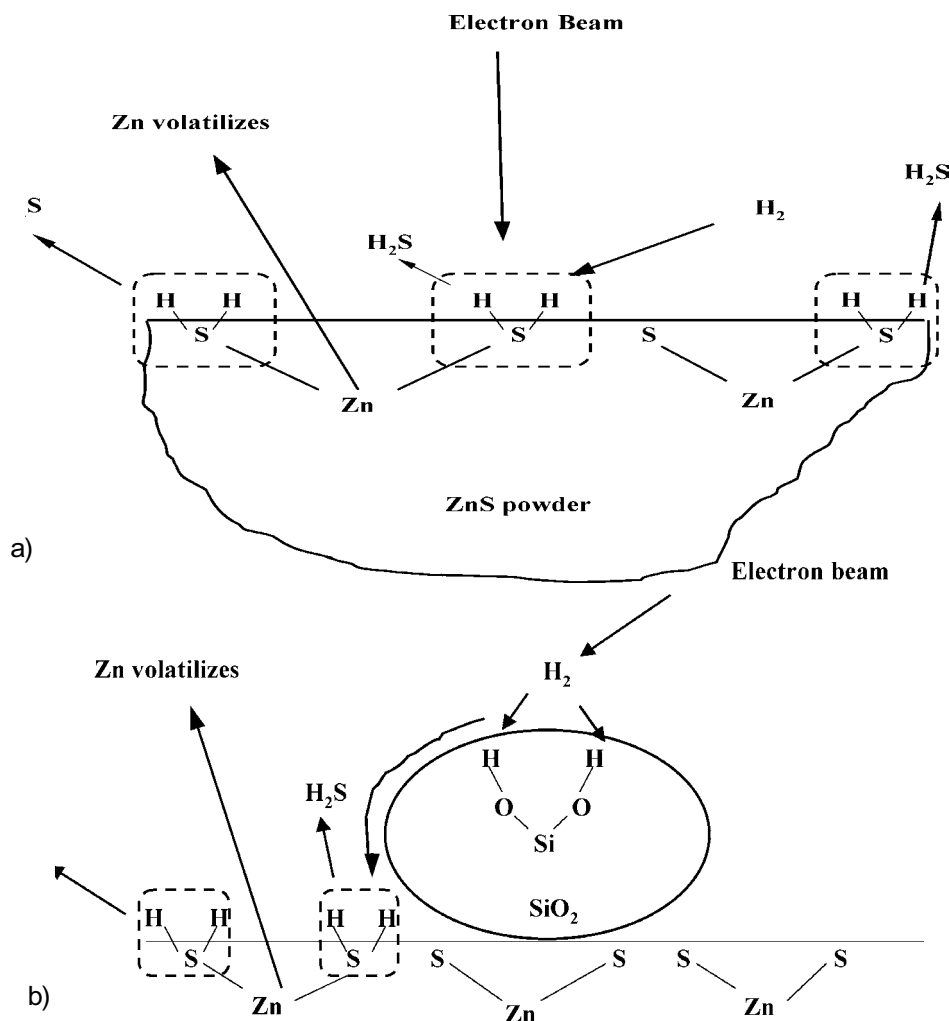


Fig. 2. ESSCR degradation model involving (a) H₂ and (b) SiO₂ nanoparticles.

a high current feed through. Another 62.7 V battery was connected in series to the first battery and then connected to a picoammeter, which was grounded.

3. RESULTS AND DISCUSSION

Degradation studies were first performed under various vacuum ambient conditions (high vs. low water partial pressure) for both the coated and uncoated ZnS:Ag,Cl phosphor samples. As reported earlier by Abrams *et al.* [2], in a vacuum with high partial pressure of H₂O (1×10^{-6} Torr), the S AES signal declined while the O AES signal increased. This was accompanied by a significant decrease in CL intensity (> 90% loss) and was indicative of the formation of an oxide layer on the surface of the phosphor. Contrary to the high water case, when the vacuum ambient was dominated by H₂ (1×10^{-6} Torr) and low H₂O content, there was no decrease in the S AES signal and no rise in the O AES signal. However, there was still an 80% decrease in CL.

Following degradation studies performed under the various vacuum ambient conditions just described, detailed SEM analysis was performed. These SEM images revealed significant surface morphological erosion. Based on Itoh's [20] suggestion that the morphology changes were related to electron beam heating, beam heating versus power density was examined. Fig. 1 shows SEM images of SiO₂-coated ZnS:Ag,Cl before degradation and after degradation at increasing power densities. As can be seen by these images, as the power density increases, the severity of the surface erosion increases until the particles are completely hollowed out at 1.4 W/cm², a phenomenon we term "ghosting". It is important to note that the erosion is always initiated at the SiO₂ nanoparticles. Also, this erosion occurs in both high and low water ambient conditions. In fact, this could, in part, explain the loss of CL in the low water, high hydrogen partial pressure case.

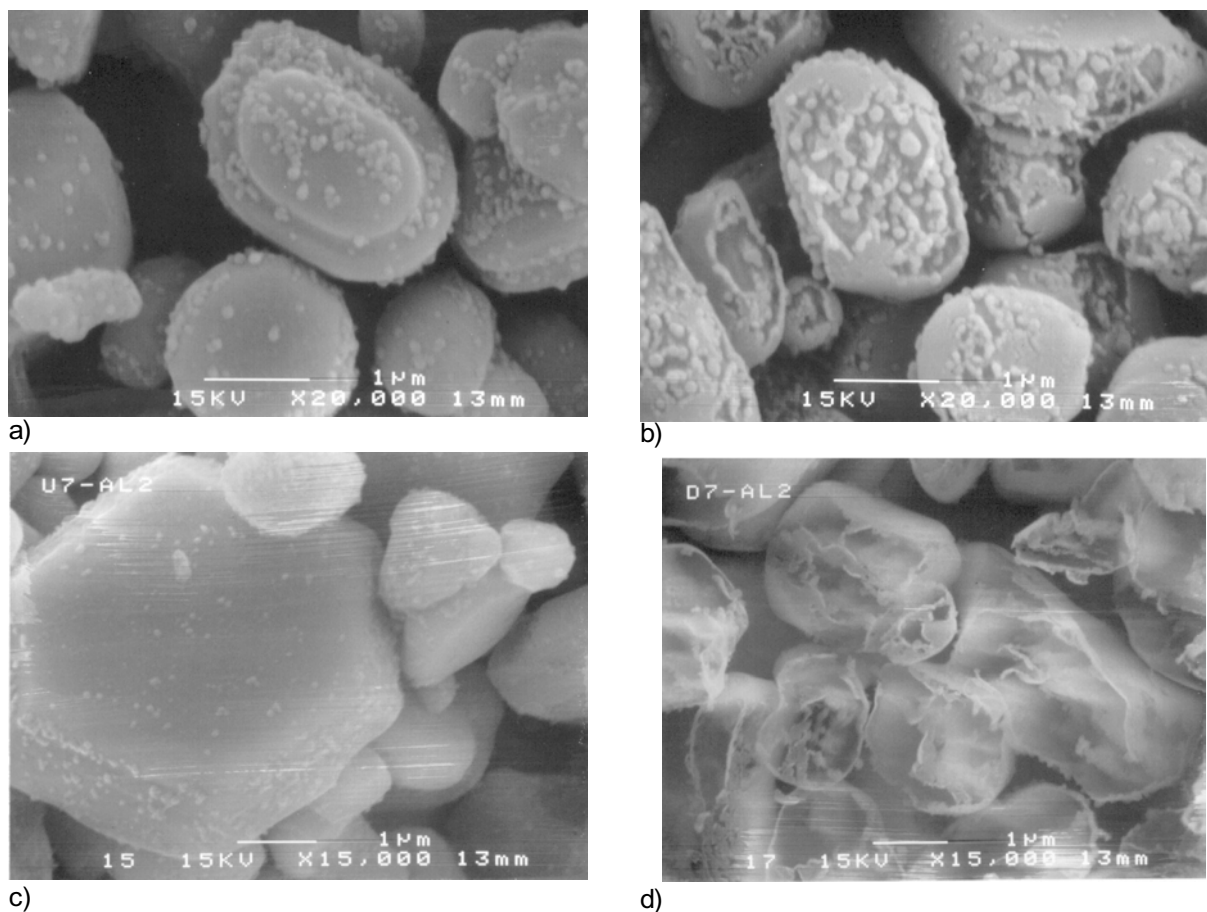


Fig. 3. SEM images of (a) (upper left) TaSi_2 -coated ZnS:Ag,Cl before degradation, (b) (upper right) TaSi_2 -coated ZnS:Ag,Cl after degradation at 0.5W/cm^2 , (c) (lower left) Al_2O_3 -coated ZnS:Ag,Cl before degradation, (d) (lower right) Al_2O_3 -coated ZnS:Ag,Cl after degradation at 0.5W/cm^2 .

No surface morphological change was observed for uncoated ZnS:Ag,Cl phosphors. Also, the extent of CL degradation was less ($< 70\%$) for these phosphors compared with the coated ones ($> 80\%$). For both coated and uncoated cases, CL degradation was worse in high water ambients than in low water. Due to the greater extent of CL degradation observed for non-uniformly coated ZnS:Ag,Cl , it is concluded that the coatings act as catalysts for degradation in both ESSCR and surface morphology. This concept is depicted in the schematic model of Fig. 2. In the case of SiO_2 , the adsorption energy for gaseous species such as H_2 or H_2O may be higher on the SiO_2 surface. The formation of OH^- groups followed by electron beam dissociation could increase the population of reactive atomic H^+ . The reactive H^+ species could travel to the small contact perimeter between the ZnS and the SiO_2 where it would react with S causing the surface reactions. The reaction with the S creates H_2S which escapes from the surface leaving Zn behind. The Zn metal may then volatilize since it has a high vapor pres-

sure under the vacuum conditions utilized and the temperatures reached due to electron beam heating ($\sim 50\text{--}100\text{ }^\circ\text{C}$). These reactions create non-stoichiometric ZnS causing a severe loss of CL intensity without a change in the spectral distribution.

Along with temperature being a factor in the surface morphology changes surface chemical reactions initiate the whole process. Morphological erosion was also observed in ZnS:Ag,Cl powders with other coatings such as TaSi_2 and Al_2O_3 . In each case, the coatings were non-uniform. In the low water cases, reactivity with H_2 was high for the Al_2O_3 case since aluminosilicate complexes may have formed. These compounds may have had an even greater catalyzing effect upon degradation. This was supported by the increased morphological deterioration observed for this case (Al_2O_3) and can be seen in Fig. 3d. The severity of surface erosion for TaSi_2 coated phosphors was not as great as for the Al_2O_3 coating. The behavior was similar to the SiO_2 case as shown in Fig. 3b. AES data suggested that very little TaSi_2 was present on the surface. The CL loss

for the TaSi₂, and Al₂O₃ coating was about 10% greater than the uncoated Osram ZnS:Ag,Cl in both the low and high water cases. The point of attack and characteristics of degradation suggest that these coatings also acted as catalysts for CL degradation and the model shown in Fig. 2 applies.

4. CONCLUSIONS

ZnS:Ag,Cl powders obtained from Kasai were non-uniformly coated with SiO₂ nano-particles. SEM images of degraded SiO₂-, TaSi₂- and Al₂O₃-coated ZnS:Ag,Cl powders revealed significant morphological damage. The extent of this damage depended upon the power density of the incoming electron beam. At low power densities of 0.4 W/cm², the erosion was minimal. When the power density was increased to 1.4 W/cm², the particles were completely hollowed, labeled as a "ghosting effect". These morphological changes are attributed to electron beam heating of the powder surface, since an increase in power results in an increase in the temperature of powder particles. The chemical reactions and surface erosion were initiated around the nanoparticles sitting on the phosphor surface.

No surface morphological change was observed for uncoated ZnS:Ag,Cl phosphors obtained from Osram Sylvania. Also, the extent of CL degradation was less (< 70%) for these phosphors compared with the coated ones (> 80%).

By coating ZnS:Ag,Cl powder phosphor with nanoparticulate particles in an attempt to decrease degradation (TaSi₂ or Al₂O₃) or facilitate processibility (SiO₂), a new mechanism for CL degradation was revealed. These discrete, non-uniform coatings acted as catalysts for degradation causing significant morphological erosion of the phosphor to occur. In all cases, the coatings increased degradation.

ACKNOWLEDGEMENTS

Sandia is a multiprogram laboratory operated by Sandia Corporation, a Lockheed Martin Company, for the United States Department of Energy under Contract DE-AC04-94AL85000.

REFERENCES

- [1] P.H. Holloway, T.A. Trottier, J. Sebastian, S. Jones, X.-M. Zhang, J.-S. Bang, B. Abrams, W. J. Thomes and T.-J. Kim // *Journ. of Appl. Phys.* **88** (2000) 1.
- [2] B. L. Abrams, W. Roos, P. H. Holloway and H. C. Swart // *Surf. Sci.* **451** (2000) 174.
- [3] H. C. Swart, J. S. Sebastian, T. A. Trottier, S. L. Jones and P. H. Holloway // *Journ. of Vacuum Science and Technology A* **14** (1996) 1697.
- [4] B. L. Abrams, L. Williams, J.-S. Bang and P. H. Holloway // *Journ. Electrochem. Soc.* **150** (2003) H105.
- [5] B. L. Abrams, *Temperature and Vacuum Ambient Effects on the Cathodoluminescent Degradation of Sulfide-Based Thin Film and Powder Phosphors*, Dissertation, Materials Science and Engineering, University of Florida, Gainesville, FL (2001).
- [6] H. C. Swart, K. T. Hillie and A. P. Greeff // *Surface Interface Analysis* **32** (2001) 110.
- [7] C. H. Seager, W. L. Warren and D. R. Tallant // *Journ. of Appl. Phys.* **81** (1997) 7994.
- [8] T. C. Candescant, *Thin CRT Technology*, Candescant Technologies Corporation website, www.candescant.com; (2001).
- [9] P. H. Holloway, B. Abrams, C. Kondoleon, S.L. Jones, J.S. Sebastian and W.J. Thomes // *Journal of Vacuum Science and Technology* **17** (1999) 758.
- [10] M. Kykta // *Information Display* (1999) 24.
- [11] S. Itoh, H. Toki, F. Kataoka, Y. Sato and K. Tamura // *Journal of SID, Supplement 1* (2000) 187.
- [12] P. H. Holloway, W. Joseph Thomes, Billie Abrams, Sean Jones and Lizandra Williams, "The Effects of Surfaces on FED Phosphors." *Proceedings of the International Display Workshop*, (2000).
- [13] A. Vecht, C. Gibbons, D. Davies, X. Jing, P. Marsh, T. Ireland, J. Silver, A. Newport and D. Barber // *Journal of Vacuum Science and Technology B* **17** (1999) 750.
- [14] B. K. Wagner, J. Penczek, S. Uang, F.-L. Zhang, C. Stoffers and C. J. Summers, *Recent Developments in Low Voltage FED Phosphors* (IDRC, Toronto, 1997).
- [15] S. W. J Kang, Soo Byung and Jae Soo Yoo // *Journal of Vacuum Science and Technology B* **15** (1997) 520.
- [16] D. B. M. Klaasen and D. M. de Leeuw // *Journal of Luminescence* **37** (1987) 21.
- [17] H. C. Swart, A. P. Greeff, P. H. Holloway and G. L. P. Berning // *Appl. Surf. Sci.* **140** (1999) 63.
- [18] H. C. Swart, L. Oosthuizen, P. H. Holloway and G. L. P. Berning // *Surface and Interface Analysis* **26** (1998) 337.

- [19] H. Bechtel, W. Czarnojan, M. Haase and D. Wadow // *Journal of the Society for Information Display* **4** (1996) 219.
- [20] S. Itoh, T. Kimizuka and T. Tonegawa // *Journ. Electrochem. Soc.* **136** (1989) 1819.
- [21] K. Kajiwara // *Journal of Vacuum Science and Technology, Part A: Vacuum, Surfaces and Films* **19** (2001)1083.
- [22] H. N. Kominami and Yoshinori Hatanaka // *Jpn. Journ. of Appl. Phys.* **35** (1996) L1600.
- [23] H. Kominami, T. Nakamura, K. Sowa, Y. Nakanishi, Y. Hatanaka and G. Shimaoka // *Appl. Surf. Sci.* **113/114** (1997) 519.
- [24] S.-H. Yang and M. Yokoyama // *Journal of Vacuum Science and Technology A - Vacuum Surfaces and Films* **16** (1998) 3443.
- [25] R. Y. K. Lee and S.S. Kang // *Journal of Luminescence* **93** (2001) 93.